In situ Raman spectroscopy study of Ru/TiO$_2$ catalyst in the selective methanation of CO

L. M. Martínez T*, A. Muñoz, M. A. Centeno, J. A. Odriozola

Departamento de Química Inorgánica – Instituto de Ciencia de Materiales de Sevilla. Centro Mixto Universidad de Sevilla - CSIC, Avda. Américo Vespucio 49, 41092 Sevilla, Spain

*leidy@icmse.csic.es

Abstract

Raman spectroscopic technique has been used to characterize a Ru/TiO$_2$ catalyst and to follow *in-situ* their structural changes during the CO selective methanation reaction (S-MET). In order to a better comprehension of the catalytic mechanism, the in situ Raman study of the catalysts activation (reduction) process, the isolated CO and CO$_2$ methanation reactions and the effect of the composition of the reactive stream (H$_2$O and CO$_2$ presence) have been carried out. Raman spectroscopy evidences that the catalyst is composed by islands of TiO$_2$-RuO$_2$ solid solutions, constituting Ru-TiO$_2$ interphases in the form of Ru$_x$Ti$_{1-x}$O$_2$ rutile type solid solutions. The activation procedure with H$_2$ at 300°C promotes the reduction of the RuO$_2$-TiO$_2$ islands generating Ru^o-Ti^{3+} centers. The spectroscopic changes are in agreement with the strong increase in chemical reactivity as increasing the carbonaceous intermediates observed. The selective methanation of CO proceeds after their adsorption on these Ru^o-Ti^{3+} active centers and subsequent C-O dissociation throughout the formation of CH$_x$/C$_n$H$_x$/C$_n$H$_x$O/CH$_x$-CO species. These intermediates are transformed into CH$_4$ by a combination of hydrogenation reactions. The formation of carbonaceous species during the methanation of CO and CO$_2$ suggests that the CO presence is required to promote the CO$_2$ methanation. Similar carbonaceous species are detected when the selective CO methanation is carried out with water in the stream. However, the activation of the catalysts occurs at much lower temperatures and the carbon oxidation is favored by the oxidative effect of water.

Keywords: Raman; CO; CO$_2$; methanation; Ru/TiO$_2$; anatase; rutile

1. Introduction

Technological procedures for production, storage, transport and distribution of hydrogen are currently under development. Therefore, research efforts in this area directed to develop distributed hydrogen production systems are an attractive approach. Hydrogen production can be obtained by hydrocarbon reforming (steam reforming, dry reforming, partial oxidation, autothermal reforming). Steam reforming favors the water gas shift reaction, thus minimizing CO, and decreases alcohol dehydration rates that produces ethylene, a source of coke that poisons the catalysts [1]. Unfortunately H_2 produced from the reformer stream carries significant amounts of H_2O, CO and CO_2. The decreasing (or elimination) of CO is mandatory if this hydrogen is used for feeding PEM fuel cells [2], since electro-catalysts as Pt and Pt-Ru are poisoned by irreversible adsorption of CO, said output must be purified to levels of CO below 50 ppm prior to admission to fuel cells.

The methanation of CO has attracted increasing interest recently because of its potential as simple technique for CO removal from H_2 -rich feed gases for fuel cells [3]. Since these gases typically contain also considerable amounts of CO_2, the reaction must be highly selective for CO methanation, with CO_2 methanation essentially being inhibited; otherwise the losses of H_2 would become intolerable. Therefore, the elucidation of the mechanism of selective methanation of CO in CO_2-rich gas mixtures as well as the reason responsible for the high selectivity are of obvious industrial importance.

The reaction pathways and mechanism of the reaction of CO or CO_2 to CH_4 as well as the nature of the active surface species are still under debate. The main question is whether the reaction starts with C-O bond breaking or with association of hydrogen and subsequent C-O bond breaking. In earlier studies, it was proposed that CO dissociates in the first step, leading to active and inactive carbon species, where the former are stepwise methanated to CH, CH_2, CH_3, and finally CH_4 [4-5]. In these studies, adsorbed CHx_{ad} species were proposed as reaction intermediates. Other studies, however, involving transient experiments, provided convincing evidence that the adsorbed CH_X species, at least those detected by IR spectroscopy, represent side products rather than reaction intermediates [6-7]. In a different concept, CO disproportionation was proposed as the initial step, followed by carbon hydrogenation to CH_4 and CO_2 reduction to CO

via the reverse water gas shift (RWGS) reaction [8]. More recent studies indicated that a formyl type (HCO)$_{[adsorbed]}$ species plays an important role in the CO methanation reaction, followed by C-O bond breaking and further hydrogenation [9-12].

The mechanism of the CO_2 methanation reaction is similarly controversial [11-13]. Following proposals of direct CO_2 methanation, it is nowadays generally accepted that $CO_{[adsorbed]}$ is the main intermediate of the CO_2 methanation [13-14]. This $CO_{[adsorbed]}$ species is subsequently hydrogenated via the mechanism for CO methanation. It has been proposed that CO_2 first reacts to $CO_{[adsorbed]}$ via the reverse water gas shift reaction, which then continues reacting to CH_4. The RWGS reaction proceeds via a formate intermediate for CO_2 conversion on supported oxides [15-17]. Studies with CO and CO_2 mixtures have shown that CO is converted almost entirely to methane before CO_2 methanation starts. In addition, dissociative CO_2 adsorption to $CO_{[adsorbed]}$ and $O_{[adsorbed]}$ and subsequent reaction of $CO_{[adsorbed]}$ to CH_4 was selected as a second alternative for the methanation of CO_2 [18].

Almost all of the studies listed in the literature focus on the hydrogenation of CO or CO_2 under conditions relevant for methane formation from synthesis gas, at nearly stoichiometric conditions (CO:H_2 1:3 or 1:4). Only a few studies deal with reaction atmospheres with a high excess of hydrogen (CO:H_2 ratios 1:20 or 1:100), as is typical for the selective methanation reaction [10,19]. The different reactant ratios have considerable effects on the reaction behavior and the dominance of a specific reaction pathway. In that sense, studies performed at low stoichiometric CO:H_2 ratios lead to mechanistic conclusions that are not necessarily relevant for the reaction under conditions typical for the selective methanation in H_2-rich reformate gases. This was the background of this ongoing study on mechanistic details of these reactions, which aims at a chemical understanding of the CO and CO_2 methanation reaction on supported Ru/TiO_2 catalysts and the underlying reasons for their selectivity in CO_2-rich reformate gases under reaction conditions typical for this process (high H_2 excess, H_2O presence, CO concentration close to 1 w.t% and atmospheric pressure). Ruthenium catalysts supported on oxides have shown good activity for methanation of CO, CO_2 and CO/CO_2 mixtures [20] compared with Pt and Pd promoting RWGS reaction. The nature of the support affects the mechanism for hydrogenation reactions of CO/CO_2, since the

metal support interaction modifies the adsorption of the intermediates as well as desorption of the products.

In the present work, we focus on the identification and characterization of the active reaction intermediates in the selective CO methanation (S-MET) reaction on a 10 wt% Ru/TiO$_2$ catalyst by *in-situ* Raman spectroscopy. Raman spectroscopy is one of the most powerful techniques for the characterization of supported metal oxide catalysts. This vibrational technique is sensitive to crystalline, amorphous, glassy or molecular as well as adsorbed species. The using of environmental Raman cells, in which the atmosphere (composition and flow), temperature and conditions are controlled, allows obtaining the spectra of the solid under real catalytic conditions, enabling time resolved *in situ* characterization of the catalyst during activation and reaction procedures, and therefore, allowing the elucidation of the catalytic mechanism.

In order to a better comprehension of the CO selective methanation reaction (S-MET), in this work, we have also studied by this technique the catalysts activation (reduction) process as well as the effect of the composition of the reactive stream (H$_2$O and CO$_2$ presence)

2. Experimental

2.1 Catalysts

Wet impregnation was selected as synthesis method. The adequate amount of Ruthenium (III) nitrosyl nitrate solution (Johnson Matthey) to obtain 13 wt % of RuO$_2$ - 87 wt % TiO$_2$ (10% Ru/TiO$_2$) was previously diluted in water (approximately 5 ml per gram support) and after added onto TiO$_2$ Aeroxide P25 (Evonik). The suspension with the support was kept under agitation for 15 min. Afterwards the solvent was removed on rotavapor and the final solid was dried at 120ºC for 30 min and calcined at 400ºC for 2h with a heating ramp of 10ºC.min^{-1}.

2.2 Raman characterization

The Raman spectra of calcined catalysts were recorded in a dispersive Horiva Jobin Yvon LabRam HR800 microscope with a He–Ne green laser (532.14 nm) working at 5 mW, and with a 600 g mm^{-1} grating. The microscope used a 50× objective and a confocal pinhole of 1000 μm. The Raman spectrometer was calibrated using a silicon wafer.

For *in-situ* Raman spectroscopy, a Linkam CCR100 cell was coupled to the Raman equipment. The microscope used a 20x objective and a confocal pinhole of 1000 μm. The catalysts were previously pretreated at 300°C using 10 mL. min^{-1} H$_2$ pure for 30 min, and then the temperature was decreased until 170°C. During this process, Raman spectra were collected at room temperature, 300°C and 170°C after 15 min of stabilization. Once at 170°C, H$_2$ was replaced by the reactive methanation mixture and the temperature was again increased until 290°C. Raman spectra were obtained each 10°C after 30 min of stabilization at each temperature under reaction conditions.

The reaction conditions were previously determined after a conventional catalytic study (not shown) of the activity and selectivity of the catalysts towards CH$_4$ production. Different methanation mixtures were studied simulating ideal streams from reforming units composed only by CO and H$_2$ or CO$_2$ and H$_2$; and real streams composed by CO, CO$_2$ and H$_2$ or CO, CO$_2$ and H$_2$ saturated in H$_2$O at room temperature. The last one simulated the most typical products from the stream of reformate reaction. The concentration of the different components of each reactive stream was fixed at 50 wt% H$_2$, 15wt% CO$_2$, 1 wt% CO and N$_2$ balance. In all cases the total reactive flow was 100 mL.min^{-1}.

3. Results and discussion

3.1 Raman study of the catalyst

TiO$_2$-P25 is a well-known and very active support in methanation reaction [21]. Its catalytic properties come from the unusual microstructure. It presents both anatase and rutile crystallographic phases in a ratio of approximately 80:20. This material does not show a simple mixture of the phases since it has been observed the coexistence of an amorphous phase and crystals of anatase and rutile disposed in layers or forming the

5

same crystal [22]. The active vibrations modes of anatase and rutile of TiO_2 are well observed by Raman spectroscopy and are modified after insertion of metallic cations. Fig 1 shows the Raman spectra of the TiO_2 support before and after incorporation of Ru. For comparison purpose the Raman spectra of commercial RuO_2 is added. The characteristic bands of anatase TiO_2 are observed at 153, 197, 397, 519 and 640 cm^{-1} and the rutile phase at 232, 447 and 612 cm^{-1}. Anatase has tetragonal structure with a cell content of two formula units (I4/amd). The atomic shifts show 18 irreducible representations that has 3 acoustic modes and 15 optic modes. The optic modes are: 1A1g + 1A2u + 2B1g + 1B2u+ 3Eg + 2Eu [23-25]. Among them only 6 Raman modes are active: A1g (515 cm^{-1}), 2B1g (397, 519 cm^{-1}) and 3Eg (144, 197, 639 cm^{-1}) [26] while Rutile has 4 Raman active modes: A1g (612 cm^{-1}), B1g (143 cm^{-1}), B2g (826 cm^{-1}) and Eg (447 cm^{-1}).

After ruthenium incorporation the anatase bands are shifted 7 cm^{-1} to the blue region (160, 204, 404, 526 and 647 cm^{-1}) while the rutile bands are shifted a new positions (258, 410 and 613 cm^{-1}) (Fig. 1). The Raman spectra of monocrystalline RuO_2 is characterized by three Raman modes: Eg, A1g and B2g at 523, 640 and 708 cm^{-1} respectively. Except the band a 708 cm^{-1} the rest of the bands overlap with the ones of anatase and their observation is difficult for Ru/TiO_2 sample (Fig. 1). The band at 708 cm^{-1} has been also related to Ti-OH or Ti-O-Ti bonds of titania nanotubes with hollandite structure [27-28]. This result would agree with the laminar structure of titania proposed for commercial TiO_2-P25 [22].

The shift of rutile bands after Ru incorporation has been explained by the mechanical strains generated from the differences between the rutile phase of RuO_2 and TiO_2 support since both have rutile structure [29]. The rutile structure of the TiO_2 is modified according to the size of the RuO_2 crystals therefore the interaction between RuO_2-TiO_2 changes and the Raman shifts are affected. Also, the wavenumber, size and intensity of the titania Raman bands have been also related to the size grain, crystallinity, partial substitution of Ti and related induced disorder that can increase defects [30]. Bersani *et al* [31-32] observed that an increase in the calcination temperature for sol-gel anatase samples decreases the wavenumber of Eg mode. Simultaneously, an increase in the domain crystalline size from 9.5 to 13.4 nm has been described to favor the shift of the bands in nanometric particles [32-33]. Golubović *et al* [33] described the factors that could

modify the position and the broadness of the Raman bands in anatase TiO_2 nano-powders, for instance: non–homogeneity of the size distribution, defects and nonstoichiometry, as well as increase of temperature. The nonstoichiometry strongly affects the vibrations modes of the lattice, as well as the symmetry of the different sites and the lattice energy, modifying the position and the broadness of the Raman bands [34]. Other factors like grain size distribution, presence of mixed phases (anatase in combination with considerable amount of rutile), solid solutions formation, and discrepancy from stoichiometry also determine the shape and shifts of the Raman bands.

Jacob and Subramanian [35] pointed out the coexistence of a TiO_2-RuO_2 solid solution with the temperature as a function of the composition of the solid. The solid solution formation is possible since cubic lattice parameters are similar for both rutile structures. a and c are 4.50 Å and 3.10 Å respectively for RuO_2, very close to the rutile phase of TiO_2, a = 4.59 Å and c = 2.96 Å with a deviation of 2% and 4.5% respectively [36]. In fact, according to the phase diagram reported by Jacob and Subramanian [35], the formation of two solid solutions RuO_2(ss) + TiO_2(ss) is favored at the compositional range of our catalyst. In good agreement, XRD data suggested the existence of both solid-solutions. After Ru incorporation, the crystalline size of anatase increased from 27 nm to 30 nm, the cubic lattice parameter decreased and the diffraction peaks of rutile of TiO_2 and RuO_2 approached, all these events are related with the formation of the RuO_2(ss) + TiO_2(ss) solid solutions. These solid solutions induce mechanical stresses that favor the shift to the blue of anatase Raman bands. From here, Ru/TiO_2 catalyst is composed by islands of TiO_2-RuO_2 solid solutions. RuO_2 particles are inserted almost exclusively in the rutile phase of TiO_2 constituting Ru-TiO_2 interphases in the form of $Ru_xTi_{1-x}O_2$ rutile type solid solutions [25,34]. In this sense, it has been reported that RuO_2 growth in an epitaxial way and produces layers of RuO_2/$Ru_xTi_{1-x}O_2$/TiO_2 ((110) plane) [37]. The islands of RuO_2-TiO_2 solid solutions modify the anatase Raman bands position thanks to the intimate contact Ru-Ti generated that affect the interaction with the rest of the phases. The formation of RuO_2-TiO_2 solid solutions with rutile structure justifies the observed shift of the bands until 258, 410 and 613 cm^{-1} (Fig. 1).

3.2 *In-situ* Raman study of the activation process

Before the catalytic reaction the catalysts were reduced with H_2. *In-situ* Raman spectra of the pretreatment of Ru/TiO$_2$ catalysts with hydrogen until 300°C is shown in Fig. 2. The anatase structure is still observed with the increase in temperature. However the intensity of the vibrations modes decreases. Furthermore a shift of the Eg band of anatase from 160 cm^{-1} to 157 cm^{-1} was observed when hydrogen passing at room temperature (Fig. S1). At 300°C this band was again shifted to the blue to 161 cm^{-1}. Then it returned to initial position of 160 cm^{-1} when the temperature decreased at 170°C. Xu *et al.* [38] studied the shift of anatase samples obtained by the sol-gel method using different surfactants. They observed that the shift to the blue and the increase in the width of Eg mode can be related to the reconstruction phenomena that produces surface atoms with higher density of the packing. This reconstruction is motived by the surfactant presence. The adsorbed species modify the coordination of polyhedron at surface level and compressive stresses can be generated. This phenomenon generates higher wavenumbers in Raman that justify the shift of the bands.

Furthermore, the reduction of RuO$_2$ to Ru^o in H_2 atmosphere also changes the normal position and width of the anatase bands. This reduction is confirmed at 300°C since the main band of Ru^o was observed at 189 cm^{-1} [39] (Fig. S1). This band was shifted to 195 cm^{-1} when the temperature decreased until 170°C. The shift observed can be related to change in particle size of Ru^o that modifies the metal/support interaction and consequently the position of Raman bands is affected. At nanoscale, the presence of oxygen vacancies can also affects the Raman features [24]. The change in the stoichiometry ratio [O]/[Ti] in nanocrystalline systems modifies the Raman spectra. This ratio is affected by the contraction and expansion of the structure after inlet and outlet of oxygen. The treatment in air decreases the variation from [O]/[Ti] ratio equal 2. However H_2 strongly affect this ratio and consequently the TiO$_2$ lattice is modified. The increase in the number of defects with the increase in temperature during reduction favors the shift to the blue and consequently the coordination polyhedron of Ti surface species is modified. The behavior described has been related with the reduction of solid solutions islands of RuO$_2$-TiO$_2$ during the pretreatment with H_2 [40]. Therefore, the activation with H_2 until 300°C promotes the ruthenium reduction, and simultaneously the number of defects increases on the support by the formation of Ti^{3+} species originated from the reduction of the RuO$_2$-TiO$_2$ islands. At the end of the reduction process, Ru^o-Ti^{3+} centers are generated [41].

3.3 Methanation of idealized CO/ H_2 mixture

Fig. 3 shows the *in situ* Raman of the catalyst during the methanation of CO from 170°C to 290°C after 30 min of stabilization in each temperature. The catalyst was previously *in-situ* preteated with hydrogen until 300ºC, after the temperature was decreased at 170ºC, from here the temperature was again increased to 290ºC under the CO/H_2 mixture. The initial spectrum under H_2 at 170ºC shows the typical bands of anatase and Ru^{o} (band at 195 cm^{-1}). However the Raman profile changes with the increase in temperature and with the reactive mixture. The band of metallic ruthenium disappears although the bands of TiO_2-RuO_2 solid solutions are observed at 270°C. These bands appear by the re-oxidation of the catalyst during the methanation reaction. However the position and intensity of these bands change with respect to the observed in Fig. 1 for Ru/TiO_2 catalyst. The new position and the high intensity of the band at 489 cm^{-1} pointed out that the solid solutions interaction with the anatase phase is affected with the reactive conditions and that the crystal size and the cubic lattice parameter are also altered. At 290ºC the Raman bands of TiO_2-RuO_2 solid solutions disappear by the reduction of the catalysts with the H_2 in the stream. The *in-situ* reduction of the catalyst is again confirmed by the observation of both the band at 195 cm^{-1} for Ru^{o} and the anatase bands at high temperature (zoom Fig. 3).

Another important feature is that the band before observed at 708 cm^{-1} in Fig 1 is now wider and has shifted to 743 cm^{-1} with the increase in temperature (Fig. 3). The band at 708 cm^{-1} has been previously related to Ti-OH [27]. The widening and shift of this band has been related with the increase of Ti-OH species promoted by the water obtained from the *in-situ* reduction of the catalyst. On the other hand the water can also favor the re-oxidation of the catalysts since the RuO_2-TiO_2 solid solutions bands are again visible.

The dehydration of the catalysts is promoted at higher temperatures. This desorption favors the formation of vacancies (defects), which are the driving force for CO methanation [21]. Zubkov *et al* [42] studied the behavior of ruthenium monocrystalline exposing the plane (109) towards the adsorption of CO. Ru (109) contains periodic double Ru atom height step defect sites, separated by 10 atom wide smooth Ru (001) terraces. They determined that the CO dissociation reaction preferentially takes place at

relatively low temperatures ($\cong$ 480 K) on the atomic step defect sites compared to smooth (001) terrace sites.

The increase in activity with the vacancies is related to the increase in the electronic interaction between the metallic particles and the reducible support. This interaction changes with the location of the ruthenium particles. The methanation reaction is sensitive to Ru size if CO dissociation is rate-limited [43]. Verykios and *col.* [20] described that the TOF values increase with the increase in the particle size in methanation reaction. Rosseti *et al.* [44] demonstrated that the selective methanation of CO is sensitive to the particle size and concentration of Ru. There is a concentration of the ruthenium in which the number of active sites is optimum. Beyond this concentration, the number of active sites decreases and the agglomeration of the metallic particles occur. Therefore, the location and size of the ruthenium particles determine the catalytic behavior for methanation reaction. Ru particles of 9 nm have been identified as the most actives ones for the CO dissociation probably by the existence of the so-called B5 sites [45]. These sites are composed by five consecutive ruthenium atoms, three of them are located in the same layer and the other two are arranged in the superior layer, forming a monoatomic step in a terrace of Ru [46]. In our case, results of XRD with the temperature in H_2 atmosphere at 300°C demonstrated that the crystal size of Ru^o particles is 8.7 nm exposing the (101) plane at $2\theta = 43.97^o$ (not shown). This crystal size is close to the reported ideal value for particles of Ru and it was also verified by TEM microscopy. This explains the high activity observed for the catalyst at higher temperatures.

Between 1000 cm^{-1} to 1800 cm^{-1} different bands of intermediate species can be observed in the spectra of Fig. 3. These bands appear at 220°C at 1119 cm^{-1}, 1356 cm^{-1}, 1504 cm^{-1} and 1595 cm^{-1}, which are normally related to carbonaceous species [45]. However the bands at 1119 cm^{-1} and 1504 cm^{-1} disappears with the increase in temperature until 250°C, while bands at 1356 cm^{-1} and 1595 cm^{-1} remains and they disappear at much higher temperature (290°C). The increase and decrease of intensity of these bands confirms that the methanation reaction is carried out through the adsorption of carbonaceous intermediates. These species are adsorbed on Ru^o-Ti^{3+} centers [41] promoted after pretreatment with H_2. Then the carbonaceous intermediates are transformed to CH$_4$ aided by the temperature and the reaction mixture since they
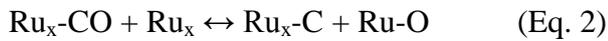
disappear at 290°C. It is suggested that the species related with the bands at 1119 cm^{-1} and 1504 cm^{-1} react more easily to CH_4 or be initial carbonaceous intermediates than the species related with the bands at 1356 and 1595 cm^{-1}, that required more temperature to complete the reaction.

Currently there is not an agreement in the literature about the assignment of the bands at 1119 cm^{-1}, 1356 cm^{-1}, 1504 cm^{-1} and 1595 cm^{-1} [39,47-49]. These bands have been usually correlated with the vibrations modes of carbon D4, D1 (Defects or disorder), D3 and G (Graphite) respectively. The G band at 1595 cm^{-1} is attributed to an ideal graphitic lattice vibration mode with E2g symmetry. The D band at 1356 cm^{-1} is induced by disorders in the graphitic lattice and its origin has been explained by double resonant Raman scattering [41,47-48]. The band at $\cong$ 1100 cm^{-1} has been also related to intermediate species with simple C-O bonds, and the band at $\cong$ 1500 cm^{-1} with normal olefins with C=C bonds [50]. The observation of the band at 1119 cm^{-1} justifies the adsorption of CO as first step in methanation reaction. Other studies have been related these bands with adsorbed intermediates like $CH_x/C_nH_x/C_nH_xO$ [51].

It has been demonstrated that the intensity ratio of D and G bands [I(D)/I(G)], or more precisely, the area ratio between them, [A(D)/A(G)], is related with the microstructure of carbonaceous materials [42]. For accurately determining the ratio [A(D)/A(G)] a curve fitting method by a combination of two Lorentzian curves is applied to the Raman spectra of Fig. 3 for the both Raman bands obtained at 250°C and 270°C. The area ratio [A(D)/A(G)] increase with the temperature from 1.60 to 2.38. This increase suggests an increase of the structural carbon disorder [41]. The less structured carbon should be easily removed from the catalytic surface by the combination of both, increase in temperature and reactive stream. In fact no Raman bands of carbon are observed beyond 270°C that confirm the transformation of the carbonaceous intermediates, probably all were hydrogenated to CH_4 at higher temperature. The no observation of carbon bands is in agreement with the microscopy results and TPD/TPO analysis of spent catalysts since no carbon deposits were observed after methanation reaction.

CO dissociation on metallic particles of Ru^o to form Ru-C and Ru-O species (Eq.1 and Eq.2) [21,41] is the first step in CO methanation on Ru/TiO$_2$ catalysts. Ru-C species react with hydrogen to form CH_4, and simultaneously Ru-O is reduced to Ru^o so that the

necessary active sites for methanation reaction are recovered. Furthermore, the H_2-rich reformate stream favors the reduction of the support close to the metallic particles to increase the number of Ru^o-Ti^{3+} centers [41], promoting in that way the CO adsorption on Ru^o. This adsorption will generate (Ti)Ru-CO species. If the reaction is through the dissociation of CO on metallic centers that generates Ru-C and Ru-O species as first step, the question is how does the mechanism work and more precisely, what types of intermediates are produced before the formation of CH_4.

$$CO + Ru_x \leftrightarrow Ru_x\text{-}CO \qquad\qquad (Eq.\ 1)$$
$$Ru_x\text{-}CO + Ru_x \leftrightarrow Ru_x\text{-}C + Ru\text{-}O \qquad (Eq.\ 2)$$

Based on the reaction pathways proposed for similar catalysts [41,52] the methanation of CO should proceed first with CO adsorption and subsequent dissociation into Ru-C and Ru-O (Eq. 2) and finally throughout the formation of CH_x/C_nH_x/C_nH_xO/CH_x-CO intermediates species that then are transformed to CH_4 in presence of CO and H_2. The simple pathway has been observed by the intervention of CH_x species of short chain to form CH_4 [42] (Eq. 3). However, the decomposition of long chain of adsorbed hydrocarbons until CH_4 has been also taken accounts [52-53].

$$C(s) \xrightarrow{H(s)} CH(s) \xrightarrow{H(s)} CH_2(s) \xrightarrow{H(s)} CH_3(s) \xrightarrow{H(s)} CH_4 \qquad\qquad (Eq.\ 3)$$
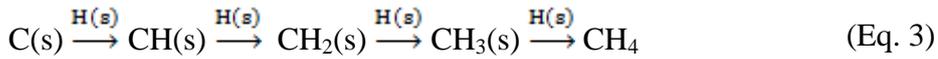
Additional Raman spectra at 220^oC were obtained during 120 min with CO/H_2 mixture to determine precisely the intermediate carbonaceous species adsorbed at low temperature in CO methanation on Ru/TiO$_2$ catalyst (Fig. 4). At t=0 new bands at 2598 cm^{-1}, 2898 cm^{-1} and 3171 cm^{-1} appear. Simultaneously the band at 1119 cm^{-1} of the adsorbed species with C-O bond is also observed which confirm the CO adsorption as a first step in methanation reaction. After 1 h of reaction the band at 2598 cm^{-1} is shifted to 2641 cm^{-1}. While the bands at 2898 cm^{-1} and 3171 cm^{-1} remain at the same position during the whole reaction. The intensities of the bands at 1119 cm^{-1} and 1504 cm^{-1} decrease with the reaction time, meanwhile at 1356 cm^{-1} and 1595 cm^{-1} increase. The high intensity of the G and D bands suggests the accumulation of the carbon and this is related to the lower capacity of the catalysts towards CH_4 formation at 220ºC, thereby its transformation requires more temperature. On the other hand, the intensity of the

band at 743 cm^{-1} increases with the time of reaction suggesting that the formation of Ti-OH species is promoted at this temperature. Higher temperatures are required to improve the reduction of the islands of RuO$_2$-TiO$_2$ solid solutions to favor the CO adsorption.

The adscription of the Raman bands detected on Fig. 4 is shown in Table 1. Bands at 1119 cm^{-1}, 1504 cm^{-1}, 2598 cm^{-1}, 2898 cm^{-1} and 3171 cm^{-1} [¡Error! Marcador no definido.2,49-51] are assigned to CH$_x$/C$_n$H$_x$/C$_n$H$_x$O/CH$_x$-CO intermediate species. CH, CH$_2$ and CH$_3$ species can form chains C-C or C=C [41,53], or join to other adsorbed species to form -OCH$_3$ (band at 1119 cm^{-1}), CO-CH$_3$ species (bands at 1504 cm^{-1} - 2898 cm^{-1}), –HCO species (band at 2598 cm^{-1}), -CH$_2$ (band at 2898 cm^{-1}) and -CH=CH$_2$ (band at 3171 cm^{-1}). The existence of these intermediates species agrees with the formation of ethane, propane, ethylene, propylene, butane, methanol, formaldehyde and ethylene described by other authors as byproducts during CO methanation [¡Error! Marcador no definido.4]. However, the analysis of the gaseous phase would be required to confirm these observations.

The adsorption and dissociation of CO on centers of Ru^o determines the catalytic behavior. Therefore, the adsorbed CH$_x$ species in combination with oxygen, from the CO dissociation, forms (Ru)-O-CH$_3$ species (band at 1119 cm^{-1}) or remains as CH$_3$-CO-(Ru) (band at 1504 cm^{-1}). Moreover, intermediates as (Ru)-HCO are also formed (band at 2598 cm^{-1}). Among them, –HCO species are the most stable since they remains longer on the catalytic surface (Fig. 4). In fact, CO is claimed to be associated with hydrogen to form metal-carbonyl hydride species (–HCO$_{[adsorbed]}$), that is one of the main intermediates in CO methanation reaction [6,52]. Results have shown that the CO is adsorbed at low temperature on metallic particles and that the rate determining step of the reaction is the breaking of the CO bond aided by H$_2$ [55]. If it is assumed, H-aided C-O bond breaking is a key step in methanation on these catalysts. After that dissociation, CH$_x$ species are obtained that then react with OH$_x$ to CH$_4$ (Eq.4). This way, if H$_2$ favors the C-O scission, the dissociation of CO from (Ru)-CO-CH$_3$ species should generate chain of CH$_{x[adsorbed]}$ (band at 2898 cm^{-1}), which leads to CH$_4$ after consecutives reactions. The carbon dissociated can be joined to –O-CH$_3$ species and forms CO-CH$_3$ intermediates (band at 1119 cm^{-1} for C-O-C bonds).

$$CO + 2H \rightarrow (CHOH) \rightarrow CH_x + OH_x \rightarrow CH_4 + H_2O \qquad \text{(Eq. 4)}$$
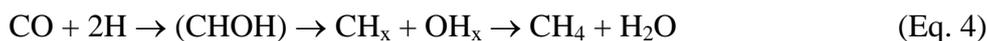
On the other hand, the band at 3171 cm^{-1} suggests the adsorption of -CH=CH$_2$ species, that can react with H$_2$ to produce ethylene (CH$_2$=CH$_2$). Ethylene is a carbon promoter [56]. Accordingly at high reaction times, a high accumulation of carbon deposits and a decreasing of Ru^o bands are observed (Fig. 4).

O$_{[adsorbed]}$ from the CO dissociation plays two roles, the first one in promoting the re-oxidation of the metal, and the second one in favoring the oxidation of the generated carbon to produce CO$_2$. This last would explain the no observation of the Raman bands of carbon at higher temperatures since carbon can be oxidized by the O$_{[adsorbed]}$. Simultaneously, both the hydrogen in the stream and the increase in temperature, can recover the active center of Ru^o which are necessary for the adsorption of CO. Although the methanation capacity decreases when the active centers are blocked by carbon, at high temperatures the oxidation of carbon by the oxidative action of O$_{[adsorbed]}$ simultaneously occurs since no Raman bands are observed between 900 cm^{-1} and 1800 cm^{-1}.

Therefore, these *in situ* Raman results showed that the first step in the methanation of CO on Ru/TiO$_2$ catalysts is the adsorption and dissociation of CO on Ru^o in Ru^o-Ti^{3+} centers to form (TiO$_2$)Ru-CO species as was described before [41]. Consequently RuC and RuO species are produced. RuC favors the formation of CH$_x$ intermediates, after the formation of carbon (bands at 1356 cm^{-1} and 1595 cm^{-1}). Then all the carbon is transformed into intermediates species at higher temperatures, that react until CH$_4$, or ultimately the carbon would react with O$_{[adsorbed]}$.

However for CO$_2$ methanation the results are totally different. Beyond 1000 cm^{-1} no Raman bands were observed (Fig. S2). Some studies have shown [17,41] that after CO$_2$ dissociation, CO$_{[adsorbed]}$ and O$_{[adsorbed]}$ are produced at temperatures as lower as 50°C [51]. If the concentration of CO$_2$ is high, the concentration of O$_{[adsorbed]}$ increases with the subsequent re-oxidation of the metallic phase decreasing the activity of the catalysts. The no observation of Raman bands associated to carbonaceous intermediates during the whole reaction with CO$_2$/H$_2$ demonstrates the low activity capacity towards CO$_2$ methanation with this catalyst.

3.4 Selective methanation of CO in CO/CO$_2$/H$_2$ mixture

In-situ Raman spectra of the methanation of CO in CO/CO$_2$/H$_2$ mixtures until 290°C after 30 min of stabilization at each temperature are shown in Fig. 5. The typical bands of the support are observed at lower reaction temperatures (170°C). At 190°C the intensity of these bands decreases although bands of carbonaceous intermediates appear. Between 190°C and 240°C, typical D and G bands from the carbon graphite are observed at 1356 cm^{-1} and 1595 cm^{-1}. Again the [A(D)/A(G)] area ratios increase with the increase in temperature from 1.10 at 190°C until 1.18 at 240°C. This result demonstrates that the deposited carbon is less structured and easily to be removed at higher temperatures. In fact, at 250°C the carbon is totally transformed and the bands of the RuO$_2$-TiO$_2$ solid solutions islands are again observed at 258 cm^{-1} and 410 cm^{-1} (Fig. 5). At much higher temperatures these bands disappear and the anatase bands are again observed. The presence of carbonaceous species show that the dissociation of CO$_2$ or CO towards C$_{[adsorbed]}$, O$_{[adsorbed]}$ and CO$_{[adsorbed]}$ occur. The presence of O$_{(adsorbed)}$ promotes the re-oxidation of Ru and the formation of RuO$_2$-TiO$_2$ islands. Only at high temperature these islands are again reduced and the anatase spectrum is recovered by the action of hydrogen of the stream

The presence of intermediates species during the methanation of CO and CO$_2$ points out a mechanism in which the CO presence favors the CO$_2$ methanation, since no reaction intermediates were observed in methanation of only CO$_2$ (Fig. S2). Moreover the CO/CO$_2$ mixture is more reactive than the idealized stream with only CO, since the formation and transformation of intermediates species occurs at lower temperatures. With CO and CO$_2$ the modification of the catalyst due to the adsorption of the intermediates species from the methanation reaction begins at 190°C (Fig. 5) with respect to 220°C for idealized CO stream (Fig. 3). Also the intermediates are totally transformed at lower temperature, 250°C with respect to 270°C for the idealized mixed CO/H$_2$ where the life time of these species is apparently greater.

Some studies have shown that the methanation of CO$_2$ occurs after the complete transformation and dissociation of CO. CH$_4$ is mainly produced throughout the hydrogenation of CO$_2$ in CO/CO$_2$ atmospheres [17]. DRIFTs experiments with CO and CO$_2$ mixture on Rh catalyst [54] showed that the adsorption/dissociation of CO$_2$ is

carried out on metallic centers to produce Rh-CO and Rh-$(CO)_2$ species. Rh-$(CO)_2$ are instable and dissociate until $CO_{[adsorbed]}$ and $O_{[adsorbed]}$. In turn, the $CO_{[adsorbed]}$ is dissociated on metallic centers until $O_{[adsorbed]}$ and $C_{[adsorbed]}$. Therefore the number of Ru-C and Ru-O sites increase after CO_2 dissociation more than after CO dissociation. $O_{[adsorbed]}$ favors the Ru re-oxidation since the RuO_2-TiO_2 island formation is observed. However, CO and H_2 decrease this effect and the metal reduction is favored [17]. Therefore H_2 and CO presence increase the available RuC and RuO since the Ru^o-Ti^{3+} centers for adsorption/dissociation of CO $((TiO_2)Ru$-CO$)$ are promoted.

At temperatures higher than 270^oC the formation of CO throughout the RWGS reaction can occur [7,43]. The formed CO can be adsorbed on metallic centers and the Ru-CO centers are increased. Simultaneously the number of Ru^o sites is increased by CO reductive action. Therefore Ru-C and Ru-O centers are favored which after are transformed into CH_4 by an associative mechanism with hydrogen [57]. This result and the observed increase in the disorder of the structural carbon favor the methanation mechanism.

The same bands that those observed for CO methanation in Fig. 4 (table 1) were distinguished for CO and CO_2 mixture methanation in the high Raman spectra region. These bands correspond to *(Ru)*-O-CH_3, CH_3-CO-*(Ru)*, *(Ru)*–HCO and CH=CH_2 intermediates. The formation of these intermediates confirms the dissociation of CO on metallic centers before the formation of CH_4. Other authors have suggested the CO and CO_2 methanation proceeds throughout the formate formation [15-17], which after are decomposed until CO to produce CH_4 with H_2. In our case the no observation of the typical raman wavenumber of formiate at ≈ 2950 cm^{-1} is in agreement with other studies in where the CO_2 methanation is due exclusively via RWGS reaction [17] and the formates can be spectator of the reaction [58]. While the CO methanation occurs throughout and associative and dissociative mechanism on metallic centers [41]. CO decreases the re-oxidation of the metal increasing the Ru^o sites. $CO_{[adsorbed]}$ can come from CO of the stream, or from the adsorption and dissociation of CO_2 at lower temperatures, or it can be generated at higher temperatures by the contribution of RWGS reaction. Anyway Ru-CO centers increases when CO and CO_2 simultaneously react with H_2-excess in the methanation reaction.

3.5 Selective methanation of CO in $CO/CO_2/H_2/H_2O$ mixtures

Fig. 6 shows the Raman spectra of CO and CO_2 methanation with water in the reaction mixture. In these more realistic conditions the modification of the catalyst starts at lower temperature with respect to the dry conditions. The D band at 1356 cm^{-1}, G band at 1595 cm^{-1}, and $-CH_x$ intermediates bands at 1119 cm^{-1} and 1504cm^{-1} are visible from 170°C with respect to 190°C (Fig. 5) for dry conditions. In this last case the area ratios between the D and G bands are lower with respect to the obtained with water, for instance at 240ºC the [A(D)/A(G)] ratios are 1.18 and 2.33 for dry and wet conditions respectively. The increase of [A(D)/A(G)] ratio in wet conditions demonstrates that both the temperature and the increasing reductive/oxidative condition of the reaction mixture $H_2O/H_2/CO$ promotes the formation of carbon less structured and more easily transformed. Both, oxidative role of water and reductive role of CO were confirmed after passing a mixture composed of H_2O/N_2 over a catalyst during 60 min (Fig. S3b). The catalyst was previously activated 120 min with CO/N_2 mixture at 170°C (Fig. S3a). The intensity of the carbon Raman bands increased with the time when CO was used, simultaneously Raman bands associated to RuO_2-TiO_2 solid solutions were also visible. At 120 min the typical Raman band of Ru^0 (195 cm^{-1}) slightly increased, which was in agreement with the reductive role of CO [17]. On the other hand, the bands associated with the deposited carbon disappeared after passing H_2O during 60 min (Fig. S3b).

Additional Raman spectra were obtained to identify the intermediates of the reaction when water is used at 170°C and at 190°C at different times by passing $CO/CO_2/H_2/H_2O$ mixture (Fig.7). For comparative purposes the Raman spectrum for CO and CO_2 methanation in dry conditions from Fig. 5 at 170°C is shown in the same figure. As said before, with water the modification of the catalyst starts at lower temperature. The bands related with intermediates species between 1000 cm^{-1} and 4000 cm^{-1} are not observed in the spectrum without water at the same temperature. In presence of water different intermediates of reaction are observed. At t=0 bands at 1119 cm^{-1}, 1504 cm^{-1}, 2136 cm^{-1} and 2956 cm^{-1} are detected without typical Raman band of the graphite carbon. The new band observed at 2136 cm^{-1} has been related to M-CO species with M = metal [51]. This result confirms the adsorption of CO on Ru^O centers forming Ru-CO centers which explains the methanation reaction throughout the formation of Ru-C and Ru-O species after CO and CO_2 dissociation. Bands at 2136 cm^{-1} of Ru-CO and at 2956

17

cm^{-1} of formates suggests both the CO adsorption over metallic center and the role of water in favoring the adsorption of formate species respectively. Concerning to the last band, it disappears after 20 min of reaction that confirms the role as spectators of the raction [52].

At t=0 min the high intensity of the bands at 1119 cm^{-1} and 1504 cm^{-1} (Fig. 7) point out the faster adsorption/dissociation of CO_2/CO on metallic centers to form Ru-CO and Ru(CO)$_2$ [54] as the first step in methanation reaction with Ru/TiO$_2$ catalyst. These intermediates are dissociated to produce Ru-C and Ru-O intermediates. As was observed for methanation of CO/CO_2 in dry conditions both Ru-C and Ru-O can react to produce *(Ru)*-O-CH$_3$ and CH$_3$-CO-*(Ru)* adsorbed species (Table 1). The faster formation of these species is due to the increase of the Ru-CO centers by both the CO and CO_2 dissociation and higher activity at lower temperature promoted by the water and H$_2$-excess.

At t=20 min the band at 2598 cm^{-1} of *(Ru)*-HCO is again observed (Fig. 7), so that hydrogen (and water) favors the dissociation of CO to form more Ru-C and Ru-O active centers. These centers are involved in the formation of CH$_x$ intermediates. After 40 min of reaction this band is still observed, while bands of *(Ru)*-O-CH$_3$ and CH$_3$-CO-*(Ru)* disappear. Simultaneously D and G graphite carbon bands are observed at 1356 cm^{-1} and 1595 cm^{-1}, and then are preserved when the temperature is increased until 190°C. In fact the spectrum obtained at 190°C is similar to the one at 170°C. It suggests that more temperature is required to transform all the carbonaceous intermediates produced.

With water, the mechanism for methanation reaction of CO and CO_2 is quite similar to the observed with dry conditions since similar intermediates species are produced. However, the activation of the catalysts occurs at much lower temperatures than without water. Moreover, the carbon oxidation is favored by the oxidative effect of water. So that, in methanation reaction on reducible Ru/TiO$_2$ catalyst there is an equilibrium between both the reducible species promoted by the simultaneously presence of CO and the excess of H$_2$ from the stream, and the oxidative species promoted by O$_{[adsorbed]}$ and water.

Once again the initial stage of the reaction is claimed to be the dissociation of CO on metallic center. Also this dissociation is promoted before the adsorption of CO_2 on Ru^0 centers. In this way Ru-CO and Ru-$(CO)_2$ centers are increased, which are then dissociated until Ru-C and Ru-O aided by hydrogen. These adsorbed intermediates can react with excess of H_2 towards methane or can be reduced to recover Ru^0 active centers respectively. Otherwise they can react with other intermediates until *(Ru)*-O-CH_3; CH_3-CO-*(Ru)* adsorbed species. These last species react with more hydrogen until CH_x CH_x / C_nH_x / C_nH_xO / CH_x-CO intermediates. Then all of them are transformed until CH_4. Thus, the mechanism involves different reaction in chain until the methane production on active centers of (TiO_2)-Ru-CO. The re-oxidation of the metallic phase can occur if the $O_{[adsorbed]}$ increase after the dissociation of CO and the island of solid solution can be observed. In this point the role of H_2/CO is crucial to again reduce the active phase and to increase the activity of the catalyst.

Conclusions

In situ Raman Spectroscopy has been demonstrated as a powerful tool for characterizing Ru/TiO_2 solids under real catalytic conditions for the selective CO methanation reaction, giving important insights concerning the catalytic mechanism.

The Raman study of the Ru/TiO_2 catalyst at room temperature shows that the solid presents islands of RuO_2-TiO_2 solid solutions with rutile structure. These islands are reduced by H_2 and temperature generating the active phase Ru^o-Ti^{3+}.

The first step in S-MET is the adsorption of CO (CO_2) on active centers (TiO_2-Ru-CO). After that, the dissociation of CO (CO_2) occurs by the action of H_2-excess. Thus, Ru-C, Ru-O, Ru-CO and Ru-$(CO)_2$ species are obtained. The active phase can be re-oxidized by $O_{[adsorbed]}$. However RuO_2 is reduced again until Ru^0 by the H_2/CO action to recover the active centers; simultaneously $C_{[adsorbed]}$ can be hydrogenated until CH_4 at higher temperatures or can be the responsible of the carbon deposits. In this sense, several CH_x / C_nH_x / C_nH_xO / CH_x-CO intermediates have been detected by Raman.

The formation of carbonaceous intermediates during the methanation of CO/CO_2 suggests that CO promotes the methanation of CO_2 since the CO methanation is firstly observed with Ru/TiO_2 catalyst.

The combination of temperature and appropriate reactive atmosphere are the paramount importance to achieve the oxidation and transformation of the carbonaceous intermediates. The CO/H_2 presence favors the reduction of RuO_2, and H_2 in excess also favors the reduction of TiO_2 close to the metal particles. Water favors the methanation at lower temperature since the carbon formed is less structured and easier to be transformed.

Acknowledgments

References

[1] P. Ramírez de la Piscina, H. Homs, *Chem. Soc. Rev*. **2008**; *37*, 2459.

[2] C. Song, *Catal. Today*. **2002**; 77, 17.

[3] S. L. Douvartzides, F. A. Coutelieris, P. E. Tsiakaras, *J. Power Sour*. **2003**; *114*, 203.

[4] S. Eckle, Y. Denkwitz, R. J. Behm, *J Catal*. **2010**; *269*, 255.

[5] N. M. Gupta, V. P. Londhe, V. S. Kamble, *J. Catal*. **1997**; *169*, 423.

[6] R. A. Dalla Betta, M. J. Shelef, *Catal*. **1977**; *48*, 111.

[7] N. M. Gupta, V. S. Kamble, V. B. Kartha, R. M. Iyer, K. R. Thampi, M. J. Gratzel, *Catal*. **1994**; *146*, 173.

[8] H. H. Nijs, P. A. Jacobs, *J. Catal.* **1980**; *66*, 401.

[9] I. A. Fisher, A. T. Bell, *J. Catal.* **1996**; *162*, 54.

[10] M. P. Andersson, F. Abild-Pedersen, I. N. Remediakis, T. Bligaard, G. Jones, J. Engbæk, O. Lytken, S. Horch, J. H. Nielsen, J. Sehested, J. R. Rostrup-Nielsen, J. K. Nørskov, I. Chorkendorff, *J. Catal*. **2008**; *255*, 6.

[11] K. Yaccato, R. Carhart, A. Hagemeyer, A. Lesik, P. Strasser, A. F. Volpe, H. Turner, H. Weinberg, R. K. Graselli, C. Brooks, *Appl. Catal. A*. **2005**; *296,* 30.

[12] J. N. Park, E. W. McFarland, *J. Catal.* **2009**; *266*, 92.

[13] H. Y. Kim, H. M. Lee, J. N. Park, *J. Phys. Chem. C*. **2010**; *114,*7128.

[14] S. Scire, C. Crisafulli, R. Maggiore, S. Minico, S. Galvagno, *Catal. Letters.* **1998**; *51*, 41.

[15] M. R. Prairie, A. Renken, J. G. Highfield, K. R. Thampi, M. J. Gratzel, *Catal.* **1991**; *129*, 130.

[16] H. Y. Kim, H. M. Lee, J. N. Park, *J. Phys. Chem.* **2010**; *114*, 7128.

[17] A. Beuls, C. Swalus, M. Jacquemin, G. Heyen, A. Karelovic, P. Ruiz, *Appl. Catal. B.* **2012**; *113–114,* 2.

[18] L. F. Liotta, G. A. Martin, G. J. Deganello, *Catal.* **1996**; *164,* 322.

[19] H. P. Bonzel, H. J. Krebs, *Surf. Sci.* **1980**; *91*, 499.

[20] P. Panagiotopoulou, D. I. Kondarides, X. E. Verykios, *Appl. Catal. B.* **2009**; *88*, 470.

[21] P. Panagiotopoulou, D. I. Kondarides, X. E. Verykios, *Appl. Catal. A.* **2008**; *344,* 45.

[22] R. I. Bickley, T. Gonzalez-Carreno, J. S. Lees, L. Palmisano, R. J. D. Tilley, *J. Sol. State Chem.* **1991**; *92,* 178.

[23] D. Medoukali, P. Hubert Mutin, A. Vioux, *J. Mat. Chem.* **1999**; *9*, 2553.

[24] B. K Sarma, A. R Pal, H. Bailung, J. Chutia; *J. Alloys. Compd.* **2013**; *577*, 261.

[25] J. M. González Carballo, E. Finoccio, S. García-Rodríguez, M. Ojeda, J. L. G Fierro, G. Busca, S. Rojas, *Catal. Today*. **2013**; *214*, 2.

[26] R. J. Gonzalez, R. Zallen, H. Berger, *Phys. Rev. B – Cond. Matter and Mat. Phys.* **1997**; *55,* 7014.

[27] K. R. Zhu, Y. Yuan, M. S. Zhang, J. M. Hong, Y. Deng, Z. Yin, *Sol. State Comm.* **2007**; *144*, 450.

[28] Y. M. Chen, A. Korotcov, H. P. Hsu, Y. S. Huang, D. S. Tsai, *New J. Phys.* **2007**; *9*, 130.

[29] D. Barkhuizen, E. Viljoen, C. Welker, M. Claeys, E. van Steen, J. C. Q Fletcher, *Pure Appl. Chem.* **2006**; *78*, 1759.

[30] A. Kremenović, B. Antić, J. Blanuša, M. Čomor, P. Colomban,L. Mazerolles, E. S. Bozin, *J Phys. Chem C*. **2011**; *115*, 4395.

[31] D. Bersani, P. P. Lottici, X. Z. Ding, *Appl. Phys. Letters*. **1998**; *72*, 73.

[32] D. Bersani, G. Antonioli, P. P. Lottici, T. Lopez, *J. Non-Crystal. Sol*. **1998**; *232-234*, 175.

[33] A. Golubović, M. Šćepanović, A. Kremenović, S. Aškrabić, V. Berec, Z. Dohčević-Mitrović, Z. V. Popović, *J. Sol-Gel Sc. Tech*. **2009**; *49*, 311.

[34] W. F. Zhang, Y. L. He, M. S. Zhang, Z. Yin, Q. Chen, *J. Phys D: Appl. Phys*. **2000**; *33*, 912.

[35] K. T. Jacob, R. Subramanian, *J. Phase Equilib. Diffus*. **2008**; 29, 136.

[36] B. H. Park, J. Y. Huang, L. S. Li, Q. X. Jia, *Appl. Phys. Letters*. **2002**; *80*, 1174.

[37] G. A. Rizzi, A. Magrin, G. Granozzi, *Phys. Chem. Chem. Phys*. **1999**; *1*, 709.

[38] C. Y. Xu, P. X. Zhang, L. Yan, *J. Raman Spect*. **2001**; *32*, 881.

[39] F. Xiao, M. Ichikawa, *Langmuir*. **1993**; *9*, 2963.

[40] A. Li Bassi, D. Cattaneo, V. Russo, C. E. Bottani, E. Barborini, T. Mazza, P. Piseri, P. Milani, F. O. Ernst, K. Wegner, S. E. Pratsinis, *J. Appl. Phys*. **2005**; *98*, 074305.

[41] P. Panagiotopoulou, D. I. Kondarides, X. E. Verykios, *Catal. Today*. 2012; *181*, 138.

[42] T. Zubkov, G. A. Morgan, J. T. Yates, *Chem. Phys. Letters*. **2002**; *362*, 181.

[43] S. Dahl, E. Tornqvist, I. Chorkendorff, *J. Catal.* **2000**; *192*, 381.

[44] I. Rosseti, L. Forni, *Appl. Catal. A*. **2005**; *282*, 315.

[45] J. M. González Carballo, J. Yang, A. Holmen, S. García-Rodríguez, S. Rojas, M. Ojeda, J. L. García-Fierro, *J. Catal*. **2011**; *284*, 102-108.

[46] R. A. Van Santen, M. M. Ghouri, S. Shetty, E. M. H. Hensen, *Catal. Sci. Tech*. **2011**; *1*, 891.

[47] Y. Kameya, K. Hanamura, *Chem. Eng. J*. **2011**; *173*, 627.

[48] N. P. Ivleva, A. Messerer, X. Yang, R. Niessner, U. Pöschl, *Environ. Sci.Technology*. **2007**; *41*, 3702.

[49] C. Li, P. C. Stair, *Catal. Today*. **1997**; *33*, 353.

[50] Y. T. Chua, P. C. Stair, *J. Catal*. **2003** ; *213*, 39.

[51] G. Socrates, *Infrared and Raman Characteristics Group Frequencies.Tables and Charts*, Los Angeles, Ed. Wiley, **2001**.

[52] A. Karelovic, P. Ruiz, *Appl. Catal. B*. **2012**; *113-114*, 237.

[53] H.Yamasaki, Y. Kobori, S. Naito, T. Onishi, K. Tamaru, *J. Chem. Soc. Faraday Trans. Phys. Chem. Cond. Phases*. **1981**; *77*, 2913.

[54] M. Jacquemin, A. Beuls, P. Ruiz, *Catal. Today*. **2010**; *157*, 462.

[55] I. Chorkendorff, M.P. Andersson, E. Abild-Pedersen, I. N. Remediakis, T. Bligaard, G. Jones, J. Engbwk, O. Lytken, S. Horch, J. H. Nielsen, J. Sehested, J.R. Rostrup- Nielsen, J. K. Norskov, *J. Catal*. **2008;** *255*, 6.

[56] M. Araque, L. M. Martínez T, J. C. Vargas, M. A. Centeno, A. C. Roger, *Appl. Catal. B*. **2012**; *125*, 556.

[57] B. H. Sakakini, *J. Mol. Catal A*. **1997**; *127*, 203.

[58] J. G. Ekerdt, A. T. Bell, *J. Catat*. **1979**; *58*, 170.

Figures Label

Fig. 1. Raman spectra of TiO_2-P25 support before and after Ru incorporation. Raman spectrum of commercial RuO_2 is also included.

Fig. 2. *In situ* Raman spectra of Ru/TiO_2 before and after reduction with H_2.

Fig. 3. *In situ* Raman spectra for methanation of idealized CO/H_2 mixture.

Fig. 4. *In situ* Raman spectra for methanation of idealized CO/H_2 mixture at 220^oC as a function of reaction time.

Fig. 5. *In situ* Raman spectra for methanation of CO and CO_2 mixture.

Fig. 6. *In situ* Raman spectra for methanation of CO and CO_2 with water in the mixture.

Fig. 7. *In situ* Raman spectra for methanation of CO and CO_2 with water in the mixture at 170^oC and at 190^oC as a function of reaction time.

Fig. S1. *In situ* Raman spectra of Ru/TiO_2 before and after reduction with H_2. Zoom between 120 cm^{-1} and 220 cm^{-1}.

Fig. S2. *In situ* Raman spectra for methanation of idealized CO_2/H_2 mixture.

Fig. S3. Effect of water at 170^oC. *In situ* Raman spectra with (A) CO/N_2 during 120 min before (B) H_2O/N_2 during 60 min.

Table 1. Raman ==wavenumbers== between 1000 cm^{-1} and 4000 cm^{-1} for Fig. 5

Intermediates species	Raman shifts (cm^{-1})
C-O-C -CH$_3$ -O-CH$_3$ C-C	1119
CH$_3$-CO C=O C=C	1504
-HCO	2598
-C=O	2898
CH$_3$-CO -C=O -CH$_3$ (aliphatic) -CH$_2$ (aliphatic – weak Raman band)	2898
-CH=CH$_2$ C=C	3171